Value at Risk (VaR) Estimation with Classical Monte Carlo and Iterative Quantum Amplitude Estimation (IQAE)

Parth Danve, Shai Verma, Edson Signor, Pranay Kakkar, Manyata Pathania
University of Connecticut, Storrs, CT

Code repository: GitHub (UConn-Quantum-Computing / MIT-iQuHack-2026-State-Street-Classiq)

***Abstract*— We study Value at Risk (VaR), defined as the α-quantile of a return distribution with $\alpha = 1 - c$ at confidence level c, and compare classical Monte Carlo estimation to a quantum workflow based on Iterative Quantum Amplitude Estimation (IQAE). Classically, VaR is computed from i.i.d. samples via the empirical quantile, exhibiting the expected $O(1/\varepsilon^2)$ sample complexity for additive accuracy ε. Quantumly, we discretize a controlled return model on a power-of-two grid, amplitude-load the resulting probabilities into an n-qubit state, and use a threshold oracle to mark tail events. IQAE estimates tail probabilities with $O(1/\varepsilon)$ oracle-query scaling, and a monotone search inverts the discrete CDF to recover VaR. We benchmark scaling and analyze sensitivity to estimator precision and discretization resolution.**

***Index Terms*— Value at Risk (VaR); Conditional Value at Risk (CVaR); Monte Carlo simulation; quantum amplitude estimation (QAE); iterative quantum amplitude estimation (IQAE); quantum risk analysis; tail probability estimation; discretization error; bisection search; Classiq SDK.**

I. INTRODUCTION

Risk management is most about the tail i.e. not what "usually" happens, but what can go wrong with small probability. *Value at Risk (VaR)* is a standard way to summarize that tail risk. Over a fixed horizon (e.g., one year) and confidence level c (e.g., 95%), VaR is determined by a left-tail return threshold that is crossed only $\alpha = 1 - c$ of the time.

Let R denote the random return over the horizon and let F_R be its cumulative distribution function. In this report we define the VaR *in return units* as the α-quantile of R:

$$r^\star = F_R^{-1}(\alpha), \qquad \text{so that} \qquad \Pr(R \le r^\star) = \alpha, \quad (1)$$

with $\alpha = 1 - c$. For example, at $c = 95\%$ we have $\alpha = 0.05$, and $r^\star$ is the *5th percentile of returns* - If one wishes to report a positive loss number instead, one can convert via $-r^\star$ for unit notional, but throughout this work we stay entirely in return space.

To keep the problem concrete and analytically checkable, we begin with a one-dimensional Gaussian return model,

$$R \sim \mathcal{N}(\mu, \sigma^2), \qquad \mu = 0.15,\ \sigma = 0.20, \quad (2)$$

for which the VaR threshold admits a closed form:

$$r^\star = \mu + \sigma\, \Phi^{-1}(\alpha), \quad (3)$$

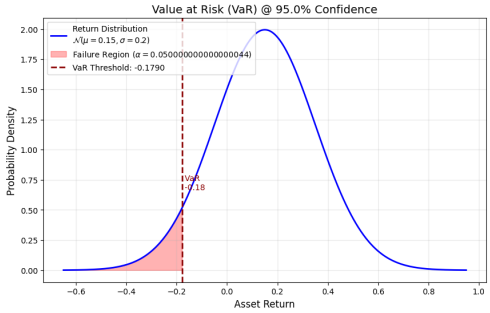

Fig. 1: VaR visualization on a Gaussian Distribution

where Φ^{-1} is the inverse CDF of the standard normal distribution. This provides a ground-truth benchmark while allowing us to focus on the algorithmic question: how efficiently can we estimate a tail probability and invert the CDF to recover the corresponding quantile threshold?

Classically, VaR is often computed via Monte Carlo simulation: draw many samples of R, sort them, and read off the empirical α-quantile. This workflow is robust and general, but converges slowly. Reducing error by a factor of 10 typically requires on the order of 100 times more samples reflecting the familiar $O(1/\varepsilon^2)$ scaling for additive accuracy ε.

On the other hand, quantum amplitude estimation reframes the same task. We discretize the return distribution onto a finite grid (mapped to 2^n basis states for n qubits), construct a threshold oracle that marks tail events $\{R \le t\}$, and use Iterative Quantum Amplitude Estimation (IQAE) to estimate tail probabilities of the form $\Pr(R \le t)$ with fewer effective "probability queries." Under idealized assumptions, we can coherently load the discretized distribution and implement the threshold oracle IQAE targets a quadratic improvement, achieving $O(1/\varepsilon)$ scaling in oracle calls for additive accuracy ε. Since VaR is an inverse problem, we wrap these tail-probability estimates inside a monotone search procedure (bisection and we later explore asymptotically faster variants such as interpolation search) to locate the index (and thus return value) whose cumulative probability matches α. In addition, we address sensitivity to discretization, estimator precision, and confidence parameters.

The Gaussian baseline is a useful starting point but is known to understate tail risk in financial returns. We therefore extend the same modeling and experimental framework to additional return distributions commonly used in risk modeling. Furthermore, we also explore *Conditional Value at Risk* (CVaR), also known as *Expected Shortfall*, as a complementary risk measure. While VaR identifies the α-quantile threshold, CVaR characterizes the *average return in the tail* beyond that threshold. This allows us to compare classical and quantum workflows not only on quantile estimation, but also on estimating tail expectations.

II. METHODOLOGY - 1D GAUSSIAN

A. Classical Monte Carlo Procedure

We first establish a classical baseline for estimating Value at Risk (VaR) using Monte Carlo simulation under a one-period Gaussian return model,

$$R \sim \mathcal{N}(\mu, \sigma^2), \qquad \mu = 0.15,\ \sigma = 0.20.$$

For a VaR confidence level c (e.g., $c = 0.95$), we denote the corresponding left-tail probability by $\alpha = 1 - c$. The VaR return-threshold is then defined as the α-quantile of R, i.e., the value $r^\star$ such that $\Pr(R \le r^\star) = \alpha$ [1]. In the Gaussian model this quantity is available in closed form:

$$r^\star_{\text{theory}} = F_R^{-1}(\alpha) = \mu + \sigma\,\Phi^{-1}(\alpha),$$

where Φ is the standard normal cumulative distribution function.

To approximate $r^\star$ via Monte Carlo with a sample budget N, we generate i.i.d. samples $R_1, \ldots, R_N$ from $\mathcal{N}(\mu, \sigma^2)$ and compute the empirical α-quantile,

$$\widehat{r}_N = \text{Quantile}_\alpha(R_1, \ldots, R_N),$$

equivalently the 100α-th percentile of the sampled returns. We quantify accuracy by the absolute deviation from the analytical benchmark,

$$\text{err}(N) = \left|\widehat{r}_N - r^\star_{\text{theory}}\right|,$$

and study how $\text{err}(N)$ decreases as a function of N. As expected from standard Monte Carlo concentration, the typical quantile estimation error scales as $\text{err}(N) = O(N^{-1/2})$ [2], [3], implying that achieving additive accuracy ε requires $N = O(1/\varepsilon^2)$ samples.

To obtain a more stable estimate of performance at each sample budget N, we repeat the Monte Carlo experiment over T independent trials, each using fresh i.i.d. draws from $\mathcal{N}(\mu, \sigma^2)$. Let $\widehat{r}_N^{(t)}$ denote the empirical α-quantile computed in trial t. We report the trial-averaged VaR estimate and the mean absolute error as

$$\bar{\widehat{r}}_N = \frac{1}{T}\sum_{t=1}^{T} \widehat{r}_N^{(t)}, \qquad \overline{\text{err}}(N) = \frac{1}{T}\sum_{t=1}^{T}\left|\widehat{r}_N^{(t)} - r^\star_{\text{theory}}\right|,$$

with $T = 50$ in our experiments. Averaging over trials reduces the variance of the reported curves and makes the convergence trend with N easier to quantify.

B. Iterative Quantum Amplitude Estimation Procedure

The key idea now is to convert the VaR quantile condition

$$\Pr(R \le r^\star) = \alpha$$

into a sequence of *tail probability* estimation problems and solve for $r^\star$ using a monotone search. In contrast to classical Monte Carlo, which estimates quantiles directly from sorted samples, the quantum method repeatedly estimates probabilities of the form $\Pr(R \le t)$ for candidate thresholds t and then inverts the CDF [6].

a) Discretizing the continuous Gaussian: Quantum circuits operate on a finite-dimensional Hilbert space, so we approximate the continuous Gaussian return distribution by a discrete distribution over $N = 2^n$ grid points, where n is the number of qubits allocated to represent the return register. We choose a truncation window around the mean,

$$[\ell, h] = [\mu - L\sigma,\ \mu + L\sigma],$$

with $L = 4$ in our experiments. This is a really good approximation since it only omits $\approx 0.0063\%$ of the distribution [9]. The uniform grid is defined as:

$$r_i = \ell + i \cdot \Delta, \qquad \Delta = \frac{h - \ell}{N - 1}, \qquad i = 0, 1, \ldots, N - 1.$$

We evaluate the Gaussian density at each grid point and normalize to obtain a discrete probability mass function

$$p_i \propto \exp\left(-\frac{(r_i - \mu)^2}{2\sigma^2}\right), \qquad \sum_{i=0}^{N-1} p_i = 1.$$

This discretization introduces an approximation error that depends on both the truncation level L (tail mass omitted outside $[\ell, h]$) and the grid resolution N (quantization within $[\ell, h]$), later we study the sensitivity of results to grid resolution.

b) Mapping discrete distribution to a quantum state: Given the discrete probabilities $\{p_i\}$, we prepare an n-qubit quantum state whose measurement statistics match the distribution:

$$|\psi\rangle = \sum_{i=0}^{N-1} \sqrt{p_i}\ \ |i\rangle\,.$$

Here $|i\rangle$ encodes the grid index i, which corresponds deterministically to the return value r_i.

c) Constructing the tail event oracle (threshold marking): To estimate $\Pr(R \le t)$ for a candidate threshold t, we operate in *index space*. For a chosen threshold index $k \in \{0, \ldots, N - 1\}$ (usually closest one to theoretical threshold) corresponding to $t = r_k$, we introduce a single-qubit indicator register and apply a reversible comparison that flips the indicator if the sampled index lies in the left tail:

$$\text{mark “good” if } i \le k.$$

After applying this marking operation to the state, the probability of measuring the indicator qubit in state $|1\rangle$ equals the inclusive discrete CDF at k:

$$a(k) = \Pr(i \le k) = \sum_{i=0}^{k} p_i. \tag{4}$$

Therefore, estimating the tail probability $\Pr(R \le r_k)$ reduces to estimating the amplitude (probability mass) $a(k)$ associated with the marked subspace [4].

d) Estimating tail probability using IQAE: Iterative Quantum Amplitude Estimation (IQAE) estimates the amplitude $a(k)$ in Eq. (4) to additive error at most ε with failure probability at most α_{fail}. In other words, IQAE returns an estimate $\widehat{a}(k)$ and a confidence interval $[a_L(k), a_U(k)]$ such that

$$\Pr(a(k) \in [a_L(k), a_U(k)]) \;\ge\; 1 - \alpha_{\text{fail}},$$
$$a_U(k) - a_L(k) \;\lesssim\; 2\varepsilon.$$

Operationally, IQAE makes a sequence of measurements using increasing numbers of Grover-operator applications (a list of integers $k_0, k_1, \ldots$, decided by a schedule). Each such "Grover depth" amplifies the marked amplitude in a controlled way, producing sharper information about $a(k)$ than naive sampling. The algorithm iteratively shrinks the confidence interval until the target precision parameter ε is met (with confidence $1 - \alpha_{\text{fail}}$).

A practical advantage of IQAE is that it avoids quantum phase estimation and instead relies on repeated sampling at different Grover iteration counts, making it more compatible with shallow-circuit constraints. In terms of *query complexity*, IQAE achieves the characteristic scaling

$$\text{oracle calls} = O\left(\frac{1}{\varepsilon}\right),$$

in contrast to classical Monte Carlo, which requires $O(1/\varepsilon^2)$ samples to achieve comparable additive accuracy on probability estimates [4], [5], [7].

e) Solving for VaR via monotone search (bisection on the index): VaR requires finding the return threshold whose tail probability equals α (e.g., $\alpha = 0.05$ for 95% VaR). In the discretized setting, this becomes finding the smallest index $k^\star$ such that

$$a(k^\star) = \sum_{i=0}^{k^\star} p_i \;\approx\; \alpha, \qquad \text{and} \qquad r^\star \approx r_{k^\star}.$$

Because $a(k)$ is monotone non-decreasing in k, we can use bisection over the index range [6]. At each bisection step we: (i) propose an index k, (ii) run IQAE to estimate $a(k)$ (and obtain its confidence interval), and (iii) move left or right depending on whether $\widehat{a}(k)$ is below or above the target α. The loop terminates when $|\,\widehat{a}(k) - \alpha\,|$ is within a preset tolerance

This search strategy separates the task into two layers: *probability estimation* (handled by IQAE) and *quantile inversion* (handled by bisection). For small grids (e.g., $n = 7$ qubits, $N = 128$ points), bisection needs at most $\log_2 N$ iterations; for higher-resolution discretizations, search dominates fewer iterations but each iteration requires a probability estimation call.

C. Interpolation Search as an alternative to Bisection Search

In our VaR workflow, the core inversion problem is to find an index $k^\star$ such that the (discrete) left-tail probability matches the target tail level α:

$$a(k) \;=\; \Pr(R \le r_k) \;\approx\; \sum_{i=0}^{k} p_i \;\approx\; \alpha, \qquad k \in \{0, \ldots, N-1\}.$$

Since $a(k)$ is monotone non-decreasing, a natural baseline is *bisection*, which is robust and guarantees convergence in $O(\log N)$ probability queries [8]. Bisection selects the midpoint of the current index interval regardless of the shape of the CDF. Interpolation search (also called the *secant* or *false-position* idea in this monotone setting) uses the fact that $a(k)$ is typically smooth and S-shaped for well-behaved distributions. Instead of choosing the midpoint, it predicts a better next index by assuming $a(k)$ is locally linear between two bracketing points.

a) Update rule: Suppose we maintain a bracket $[k_L, k_U]$ such that $a(k_L) \le \alpha \le a(k_U)$ (with $k_L < k_U$). Given current estimates $\widehat{a}(k_L)$ and $\widehat{a}(k_U)$, interpolation search proposes

$$k_{\text{new}} \;=\; k_L \;+\; \left\lfloor \frac{\alpha - \widehat{a}(k_L)}{\widehat{a}(k_U) - \widehat{a}(k_L)} \,(k_U - k_L) \right\rfloor,$$

clipped to $[k_L, k_U]$ as needed. We then evaluate $\widehat{a}(k_{\text{new}})$ (via IQAE or a classical CDF computation) and update the bracket depending on whether $\widehat{a}(k_{\text{new}})$ is below or above α.

b) When it helps: Interpolation search can reduce the number of inversion steps when:

- the grid is high-resolution (large N), so saving even a few iterations matters,
- probability estimation is expensive (e.g., each step calls IQAE), making fewer CDF queries directly valuable.

We have shown that for our current settings interpolation-style methods can converge faster than bisection (often described as $O(\log \log N)$ behavior for interpolation search), whereas bisection remains $O(\log N)$.

III. RESULTS 1-D GAUSSIAN

A. Classical Monte Carlo

Figure 2 summarizes the Monte Carlo VaR experiment for the one-year Gaussian return model with $(\mu, \sigma) = (0.15, 0.20)$ at confidence level $c = 95\%$ (i.e., $\alpha = 0.05$). For each sample size N (log-spaced from 10^2 to 10^6), we draw N i.i.d. returns, estimate the VaR as the empirical 5th percentile, and repeat over multiple independent trials to report averaged behavior.

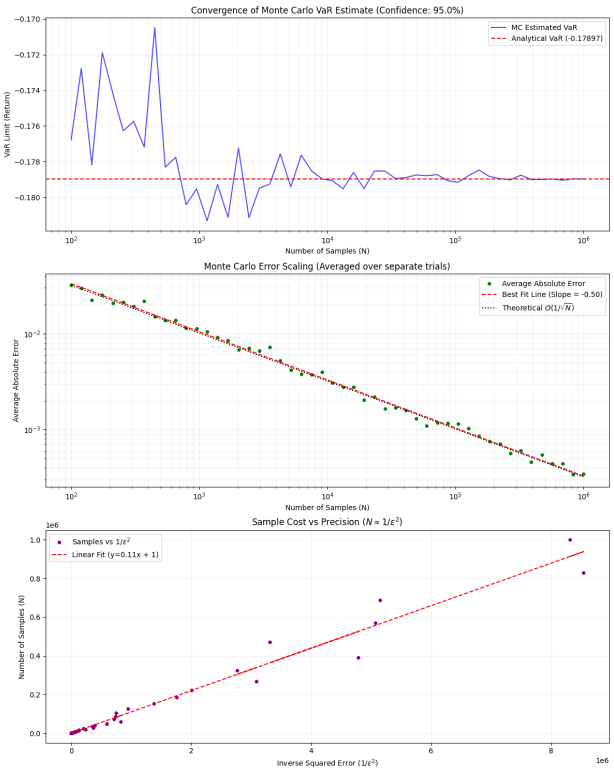

Fig. 2: Classical Monte Carlo Results

1) **VaR convergence (top panel).** The Monte Carlo estimate $\widehat{r}_N$ approaches the analytical Gaussian benchmark $r^{\star}_{\text{theory}} = \mu + \sigma\,\Phi^{-1}(0.05) \approx -0.17897$, shown as the dashed horizontal line. At small N, the quantile estimate is visibly noisy, but stabilizes as N increases.

2) **Error scaling (middle panel).** We compute the *average absolute error* $\overline{\text{err}}(N) = \mathbb{E}\left[\left|\widehat{r}_N - r^{\star}_{\text{theory}}\right|\right]$ (estimated by trial-averaging) and plot it versus N on log-log axes. The fitted slope is approximately -0.50, matching the expected Monte Carlo quantile convergence rate $\overline{\text{err}}(N) = O(N^{-1/2})$. The dotted reference curve highlights the same $O(1/\sqrt{N})$ trend.

3) **Cost vs. precision (bottom panel).** Rewriting the above as a sample-complexity statement gives the classical scaling $N = O(1/\varepsilon^2)$ for achieving additive accuracy ε in the VaR estimate. This is visualized by plotting N against $1/\overline{\text{err}}(N)^2$, which exhibits an approximately linear relationship (up to finite-sample scatter), consistent with $N \propto 1/\varepsilon^2$.

These results serve as the classical baseline: VaR estimation via sampling-and-sorting is straightforward and robust, but improving accuracy requires quadratically more samples.

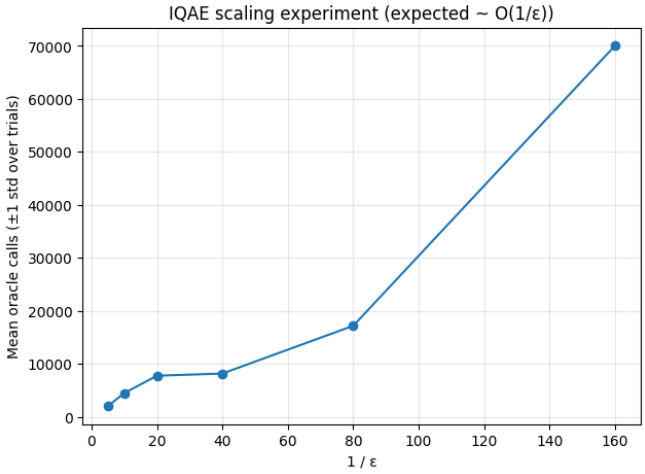

Fig. 3: Mean oracle calls versus $1/\varepsilon$ for IQAE at a fixed VaR-adjacent threshold, illustrating the expected $O(1/\varepsilon)$ query scaling.

B. IQAE

To empirically demonstrate the expected $O(1/\varepsilon)$ behavior, we fix a single threshold index k near the VaR region and repeat IQAE runs for a range of ε values taken from a geometric progression while α_{fail} is constant (Figure 3). From each IQAE run we extract a proxy for the number of oracle calls by summing, over all IQAE iterations, the number of Grover iterations used in that iteration (plus state-preparation/oracle overhead) multiplied by the number of measurement shots. Plotting the resulting oracle-call counts against $1/\varepsilon$ provides an empirical validation of the linear-in-$1/\varepsilon$ scaling predicted by amplitude-estimation theory, subject to constant overheads and simulator-dependent effects that are most visible at coarse precision targets.

To connect this query-complexity claim back to VaR estimation itself, recall that our quantum pipeline has two independent approximation knobs: (i) the *discretization* induced by representing returns on a finite grid of size $N = 2^n$, and (ii) the *estimation precision* ε used by IQAE when evaluating tail probabilities. The scaling experiment in Figure 3 isolates (ii) by holding the threshold fixed and sweeping ε while 4 does (i). In the full VaR search, each candidate threshold evaluation incurs this $O(1/\varepsilon)$ oracle cost, while increasing n reduces quantization error in the returned VaR but also enlarges the underlying state space and oracle arithmetic. These effects thus combine when solving for the VaR threshold on a discretized Gaussian grid and have the overall $1/\varepsilon$ behaviour.

C. Sensitivity to Confidence Level (c)

As shown in Figure 5, the VaR return-threshold decreases (becomes more negative) as the confidence level increases for both analytical and IQAE-based estimates. This behavior follows directly from the quantile definition: VaR at confidence c corresponds to the left-tail level $\alpha = 1 - c$, so increasing

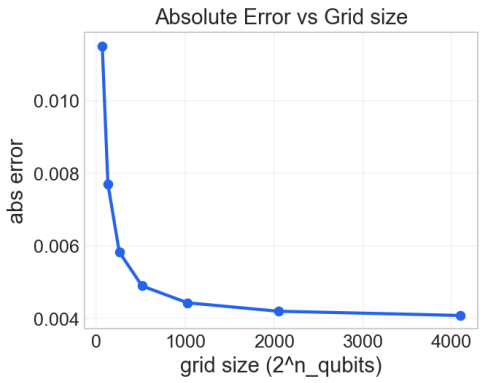

Fig. 4: Grid Size scaled with absolute error shows asymptotic $1/\varepsilon$ behaviour

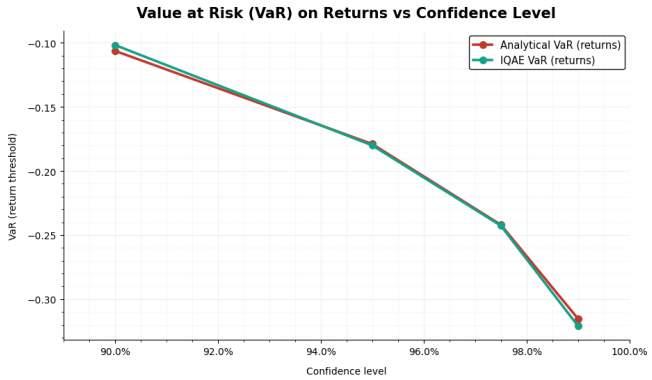

Fig. 5: Comparison of analytical and IQAE-based Value at Risk estimates shows close agreement across increasing confidence levels, with deeper negative return thresholds at higher confidence.

c reduces α and forces the cutoff deeper into the left tail. Since the CDF is monotone, smaller α implies a smaller quantile value, hence a more negative return threshold. The close agreement between the two curves indicates that IQAE accurately recovers the same tail probabilities on the discretized grid; residual differences arise from discretization and finite estimator tolerance.

D. Sensitivity to Discretization (num_qubits)

To assess the impact of grid resolution, we swept the number of qubits in the index register from $n = 6$ to $n = 10$ (corresponding to $N = 2^n$ bins) while keeping the truncation window fixed at $[\mu - 4\sigma, \mu + 4\sigma]$ and holding the IQAE/bisection settings unchanged in Figure 6. As the resolution increases, the VaR estimate shifts systematically and then stabilizes: the estimated threshold moves from approximately -0.168 at $n = 6$ toward ≈ -0.1745 by $n = 12$. In parallel, the absolute deviation from the continuous-theory Gaussian VaR decreases with n, dropping from about 1.15×10^{-2} (at $n = 6$) to $\sim 4.4\times 10^{-3}$ (at $n = 10$). The improvement per added qubit becomes noticeably smaller beyond $n \approx 8$, indicating diminishing returns from finer discretization: at higher resolutions the residual discrepancy is no longer

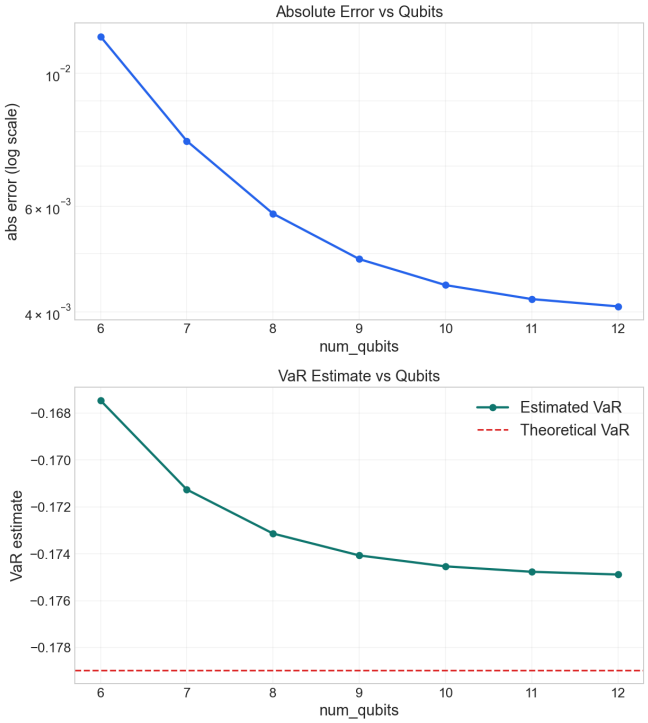

Fig. 6: VaR estimate and absolute error vs. number of qubits (resolution); dashed line marks the theoretical VaR.

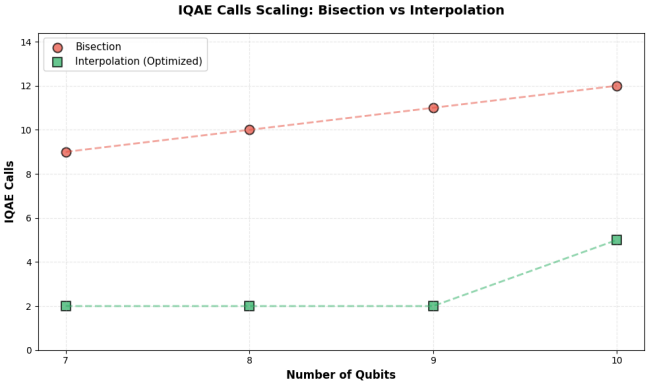

Fig. 7: Grid Resolution vs IQAE iterations

dominated by grid coarseness alone, but increasingly by non-discretization effects (e.g., truncation of the Gaussian tails and the finite precision/tolerances used in the IQAE probability estimates and the bisection stopping rule).

E. Interpolation v/s Bisection

Figure 7 shows that the interpolation strategy consistently uses fewer IQAE calls than bisection as the grid resolution increases. While bisection scales roughly linearly with the number of qubits (reflecting the worst-case $O(\log 2^n) = O(N)$ behavior), interpolation remains nearly flat over $n = 7$–9 and increases only mildly by $n = 10$. This reduction in the number of probability queries directly translates into lower overall quantum resource use.

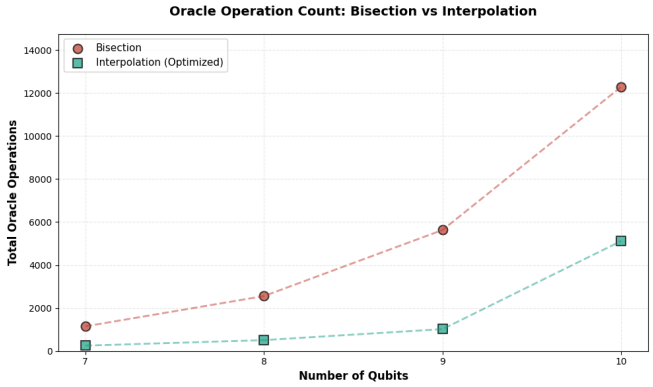

Fig. 8: Grid Resolution vs Oracle Calls

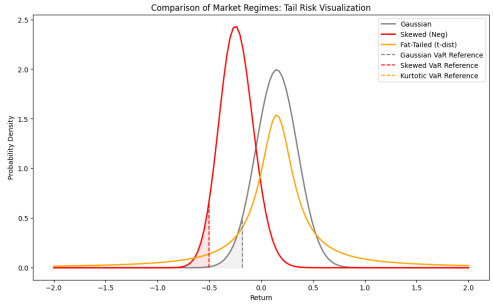

Fig. 9: The Gaussian distribution provides a thin-tailed baseline, the Student's t captures excess kurtosis through heavier tails, and the skewed distribution introduces asymmetric downside risk.

The same effect is visible in the total oracle-operation count (Figure 8). Since each IQAE call itself costs oracle applications that scale approximately as $O(1/\varepsilon)$, reducing the *number* of IQAE invocations compounds with the per-call savings. Empirically, the interpolation variant yields a multi-× reduction in total oracle operations across all tested qubit sizes, with the gap widening as resolution increases.

IV. METHODOLOGY - EXTENSIONS

A. Distributional Modeling Beyond Gaussian Assumptions

A central component of any Value at Risk (VaR) framework is the specification of the return-generating distribution. Classical risk models frequently assume that asset returns follow a Gaussian process due to its analytical tractability, closed-form moments, and compatibility with mean–variance portfolio theory. However, extensive empirical evidence from financial econometrics demonstrates that real-world return series deviate systematically from normality, exhibiting excess kurtosis, skewness, and volatility clustering. Consequently, a robust risk analysis pipeline must explicitly interrogate how distributional assumptions influence tail-risk estimates.

Under a Gaussian distribution with mean μ and variance σ^2, tail probabilities decay exponentially. This implies that extreme losses are statistically rare. In contrast, observed financial returns often display *fat tails*, meaning that the probability mass in the extremes is materially higher than predicted by a normal model. Formally, if R denotes log-returns, empirical studies frequently observe

$$\mathbb{E}\left[(R-\mu)^4\right] > 3\sigma^4,$$

indicating kurtosis exceeding that of the Gaussian benchmark. From a risk-management perspective, underestimating this tail thickness directly leads to systematically biased VaR thresholds and an undercapitalization against rare but catastrophic events.

As a reference model, returns are first parameterized as

$$R \sim \mathcal{N}(\mu, \sigma^2),$$

providing a convenient starting point for amplitude encoding due to its smooth density and well-behaved cumulative distribution function. Despite its limitations, the Gaussian approximation remains operationally useful because:

- Aggregated returns often approach normality under the Central Limit Theorem when driven by many independent micro-shocks.
- Parameter estimation is statistically efficient and computationally stable. [10]
- Many regulatory and legacy risk systems are calibrated around variance-based metrics.

Thus, the Gaussian model serves as a controlled baseline against which heavier-tailed alternatives can be evaluated.

To capture leptokurtic behavior, we generalize the return process using distributions with polynomial tail decay [11]. A canonical choice is the Student's t distribution,

$$R \sim t_\nu(\mu, \sigma),$$

where the degrees of freedom ν govern tail thickness. As $\nu \to \infty$, the distribution converges to Gaussian; for small ν, tail probabilities increase dramatically. This parameter therefore provides a natural experimental axis for stress-testing VaR sensitivity to extreme-event frequency.

From a methodological standpoint, varying ν enables a controlled deformation of the probability landscape while preserving symmetry, allowing us to isolate the impact of kurtosis on tail-threshold estimation without conflating skew effects.

Real markets additionally exhibit asymmetric downside risk driven by leverage effects, liquidity shocks, and behavioral panic dynamics. To model this asymmetry, skewed distributions are introduced through parameterized transformations that permit unequal left and right tail weights. Conceptually, this allows the loss tail to thicken independently of the gain tail, a feature that is particularly relevant for

regulatory risk metrics which focus exclusively on downside exposure.

In discretized form, these distributions are mapped onto a finite grid $\{r_i\}_{i=0}^{N-1}$ with associated probabilities $\{p_i\}$ prior to amplitude loading. Care is taken to ensure that grid resolution is sufficiently fine so that discretization error remains subdominant relative to probability-estimation error. [12]

Distributional flexibility is especially consequential in the context of amplitude-estimation-based workflows [10]. Because quantum algorithms estimate tail probabilities rather than analytic quantiles, any mis-specification of the underlying distribution propagates directly into the oracle-marked event space. Testing multiple distributional families therefore serves two methodological objectives:

1) Quantifying the robustness of VaR estimates to higher-order moment structure.
2) Evaluating whether quantum sampling advantages persist when tail mass increases and rare events become less sparse.

Each candidate distribution is parameterized, discretized onto a power-of-two grid to facilitate quantum state preparation, and normalized to produce a valid amplitude distribution. The resulting states form interchangeable inputs to the VaR search procedure, ensuring that observed differences in tail thresholds arise strictly from distributional geometry rather than algorithmic variation.

By systematically moving from Gaussian to fat-tailed and skewed return models, the methodology transitions from an analytically convenient abstraction toward a structure more representative of real financial systems. This progression enables a principled examination of how higher-order statistical features reshape the loss landscape, thereby strengthening the interpretability and external validity of the VaR framework.

B. Conditional Value at Risk (CVaR) via IQAE

While VaR identifies the left-tail threshold $r^\star$ satisfying $\Pr(R \le r^\star) = \alpha$, *Conditional Value at Risk (CVaR)* (Expected Shortfall) measures the *average return inside the tail* and is widely studied as a coherent tail-risk measure [1]. Working in return space and using a left-tail convention, we define

$$\mathrm{CVaR}_\alpha(R) \;\equiv\; \mathbb{E}[R \mid R \le r^\star], \qquad \alpha = 1 - c.$$

In our implementation, the distribution is discretized on a grid and both the tail probability and tail expectation are estimated using *Iterative Quantum Amplitude Estimation (IQAE)* [5], leveraging the amplitude estimation framework [4] used in quantum risk analysis [6].

a) Discrete return model and VaR index: We discretize a continuous return distribution onto $N = 2^n$ grid points $\{r_i\}_{i=0}^{N-1}$ with probabilities $\{p_i\}$ and prepare the amplitude-encoded state

$$|\psi_p\rangle \;=\; \sum_{i=0}^{N-1} \sqrt{p_i}\,|i\rangle\,.$$

For an index threshold k, define the discrete left-tail probability

$$\alpha(k) \;=\; \Pr(i \le k) \;=\; \sum_{i=0}^{k} p_i.$$

We first compute the VaR index $k^\star$ (and thus $r^\star \approx r_{k^\star}$) using the same monotone search described in the VaR section, where each step calls IQAE to estimate $\alpha(k)$ and compares it to the target α [5].

b) CVaR as a ratio of two tail sums: Given $k^\star$, the discrete CVaR in return units is

$$\mathrm{CVaR}_\alpha(R) \;\approx\; \frac{\sum_{i=0}^{k^\star} p_i\, r_i}{\sum_{i=0}^{k^\star} p_i} \;=\; \frac{\sum_{i=0}^{k^\star} p_i\, r_i}{\alpha(k^\star)}.$$

The denominator is a tail probability, but the numerator is a *tail expectation* (weighted sum), which must be converted into an amplitude-estimation-friendly form [4,5,6].

c) Affine normalization of returns: Because amplitude-estimation-based constructions target probabilities, we map returns to the unit interval:

$$s_i \;=\; \frac{r_i - r_{\min}}{r_{\max} - r_{\min}} \in [0,1], \qquad r_{\min} = \min_i r_i, \quad r_{\max} = \max_i r_i.$$

This gives

$$r_i = r_{\min} + (r_{\max} - r_{\min}) s_i.$$

Therefore it suffices to estimate $\mathbb{E}[S \mid i \le k^\star]$ and then convert back to returns.

d) Weighted-distribution construction: Define the global normalizer

$$Z_S \;=\; \mathbb{E}[S] \;=\; \sum_{i=0}^{N-1} p_i\, s_i,$$

and the corresponding *weighted* probability mass function

$$w_i \;=\; \frac{p_i\, s_i}{Z_S}, \qquad \sum_{i=0}^{N-1} w_i = 1.$$

Now define the left-tail probability under the weighted distribution:

$$\beta(k) \;=\; \sum_{i=0}^{k} w_i \;=\; \frac{\sum_{i=0}^{k} p_i\, s_i}{Z_S}.$$

Rearranging yields the tail sum of S:

$$\sum_{i=0}^{k} p_i\, s_i \;=\; Z_S\, \beta(k),$$

and hence the conditional mean of S inside the tail becomes

$$\mathbb{E}[S \mid i \le k] = \frac{Z_S\, \beta(k)}{\alpha(k)}.$$

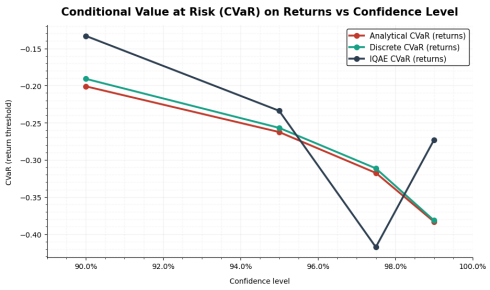

Fig. 10: Comparison of analytical, discretized, and IQAE-based CVaR estimates across confidence levels.

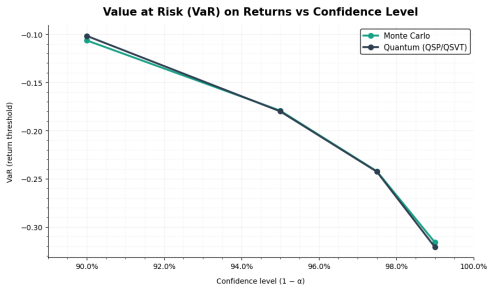

Fig. 11: Comparison of analytical, Monte Carlo, and quantum (QSP/QSVT) VaR estimates as a function of confidence level.

e) Final CVaR estimator from two IQAE calls: Operationally, at the VaR index $k^\star$ we estimate $\alpha(k^\star)$ and $\beta(k^\star)$ using IQAE [5] within the amplitude estimation framework [4], reusing the same threshold-marking oracle as in quantum risk analysis constructions [6,14]. The final CVaR estimate is computed classically from the ratio.

C. CVaR Estimation via Quantum Signal Processing (QSP/QSVT)

The IQAE-based approach estimates CVaR by reducing tail expectations to ratios of tail probabilities via amplitude estimation [4,5]. In this subsection, we describe an alternative *QSP/QSVT-based formulation* that computes tail expectations via polynomial transformations, as explored in quantum risk-analysis extensions beyond (C)VaR [13] and derivative-focused quantum risk settings [14].

a) Block-encoding of the return distribution: As before, we discretize the return distribution onto $N = 2^n$ grid points with probabilities $\{p_i\}$ and returns $\{r_i\}$ and prepare

$$|\psi\rangle = \sum_{i=0}^{N-1} \sqrt{p_i}\,|i\rangle\,.$$

This enables coherent transformations that implement tail truncation/weighting without an iterative amplitude-estimation loop [13,14].

D. Expectile Value at Risk (EVaR)

Expectiles provide an optimization-based tail-sensitive statistic that interpolates between the mean and extreme-tail behavior, and can be used to define a VaR-like threshold through asymmetric deviation balancing [13]. In our setting, EVaR is solved by root-finding on an implicit balance condition, while the required tail probabilities and tail expectations are estimated using the same quantum risk primitives as for CVaR [4,5,6].

V. Results: Extensions

A. IQAE-Based CVaR vs Confidence Level

Figure 10 reports CVaR (expected shortfall) in *return units* as a function of confidence level. The analytical and discretized curves decrease monotonically as confidence increases, consistent with CVaR conditioning on increasingly extreme tail outcomes as $\alpha = 1 - c$ shrinks [1].

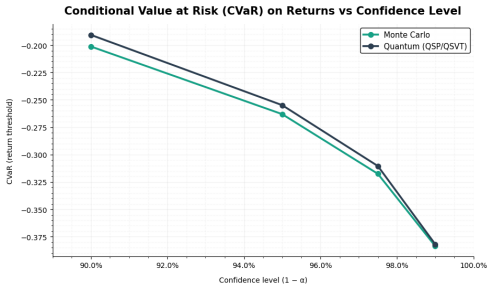

Fig. 12: Comparison of analytical, Monte Carlo, and quantum (QSP/QSVT) CVaR estimates as a function of confidence level.

IQAE is used here because CVaR decomposes into *tail probabilities and tail expectations*, both accessible through amplitude estimation [4] and its iterative variant IQAE [5], as in quantum risk analysis [6]. The localized dip around $c = 0.975$ is an estimation artifact: IQAE-CVaR uses a ratio of estimated quantities, and when α is small, additive error in the denominator and discretization-induced index changes can be amplified by division [5,6,13].

B. QSP/QSVT-Based VaR and CVaR vs Confidence Level

Figures 11 and 12 show VaR and CVaR estimates obtained using analytical formulas, Monte Carlo simulation [3], and QSP/QSVT-based quantum evaluation [13,14]. Both risk measures become more negative as confidence increases, since $c \uparrow$ implies $\alpha \downarrow$ and the tail events become rarer and more severe [1].

QSP/QSVT is used because it enables *direct polynomial transformations* that implement tail truncation/weighting coherently, providing a numerically stable alternative to ratio-based estimators in extreme tails [13,14]. For VaR (Fig. 11), the close overlap indicates accurate recovery of left-tail quantiles (with residual grid/sampling effects). For CVaR (Fig. 12), small separations reflect CVaR's higher sensitivity to the full tail average, but the quantum curve remains smooth and trend-consistent without the dip behavior seen in IQAE-based CVaR [13,14].

C. EVaR Accuracy vs Oracle Budget (IQAE)

Figure 13 shows absolute EVaR error versus an effective oracle-budget proxy. The strong initial error reduction

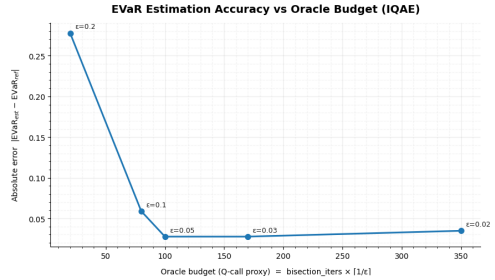

Fig. 13: EVaR estimation error versus effective oracle budget for IQAE-based estimation.

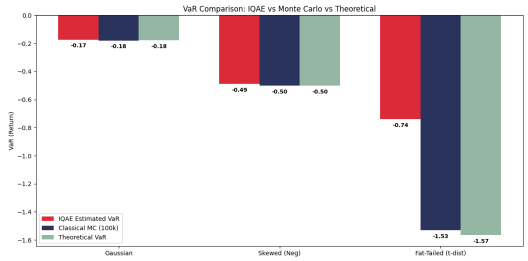

Fig. 14: Comparison of IQAE-estimated, classical Monte Carlo, and theoretical VaR across Gaussian, negatively skewed, and fat-tailed (Student's t) return distributions.

is consistent with IQAE's role as the dominant precision driver at low budgets [5], building on amplitude-estimation-based quantum speedups over classical sampling [4,7]. The flattening at larger budgets indicates saturation once IQAE error drops below discretization and root-finding tolerances. Mild non-monotonicity at the smallest ε values is consistent with finite-sample noise and the implicit (root-finding) nature of the EVaR defining condition [5,13].

D. Impact of Non-Gaussian Return Distributions on VaR

Figure 14 examines how distributional structure influences left-tail risk by comparing VaR estimates under Gaussian, negatively skewed, and fat-tailed return models. Across all methods, the magnitude of VaR increases as the distribution departs from normality, reflecting the higher probability mass allocated to extreme loss events when skewness and excess kurtosis are introduced.

Under the Gaussian specification, the three estimators closely align near -0.18, consistent with the thin-tail assumption that suppresses extreme outcomes. While analytically convenient, this behavior is known to systematically understate tail risk when markets exhibit leptokurtosis [1]. The agreement between IQAE and classical Monte Carlo further confirms that discretization and amplitude encoding recover the baseline quantile with minimal distortion.

Introducing negative skew shifts probability mass toward the loss tail, producing a substantially more conservative VaR near -0.50. This behavior follows directly from quantile monotonicity: for fixed confidence c, any redistribution of density toward the left tail must lower the threshold $r^\star$ satisfying $\Pr(R \le r^\star) = \alpha$. The close overlap between theoretical and Monte Carlo estimates suggests that the observed shift is driven primarily by distributional geometry rather than sampling artifacts.

The fat-tailed Student's t specification generates the most pronounced effect, with VaR deepening to approximately -1.5. Polynomial tail decay implies that extreme losses remain comparatively probable even far from the mean, causing the quantile function to expand rapidly relative to the Gaussian benchmark. This result is consistent with the well-documented sensitivity of VaR to kurtosis, where heavier tails amplify downside exposure despite identical first and second moments [1].

Notably, the IQAE estimate remains directionally consistent across all distribution families but exhibits a visible deviation in the fat-tailed regime. Because amplitude estimation targets rare-event probabilities, heavier tails reduce event sparsity and alter the effective amplitude landscape, increasing sensitivity to discretization resolution and threshold localization. Such behavior highlights a critical methodological point: quantum advantage pertains to sampling complexity, but the fidelity of the encoded probability model ultimately governs risk accuracy.

Overall, Figure 14 demonstrates that distributional assumptions dominate VaR behavior. Moving beyond Gaussian approximations materially changes the inferred capital threshold, reinforcing the importance of modeling higher-order moments when evaluating extreme financial risk.

VI. Discussion and Future Directions

A. When Quantum Methods Are Advantageous

Our results indicate that quantum methods become advantageous in regimes where *high-precision tail risk estimates* are required. In particular, advantages emerge when estimating small tail probabilities or tail expectations (e.g., high-confidence VaR, CVaR, and EVaR), where classical Monte Carlo methods suffer from $O(1/\varepsilon^2)$ sample complexity [3,7]. In contrast, quantum amplitude-estimation-based approaches achieve $O(1/\varepsilon)$ scaling in the target additive precision [4,5], making them asymptotically favorable for sufficiently small ε.

The advantage is most pronounced for probability-centric tasks such as VaR estimation and tail probability inversion, and for expectation-based measures (CVaR, EVaR) when they can be expressed in terms of tail probabilities and weighted expectations. QSP/QSVT-based methods further improve numerical stability in extreme tails by avoiding ratio-based estimators, making them attractive for high-confidence CVaR estimation.

B. Assumptions Enabling Quantum Advantage

The observed quantum advantage relies on several modeling and access assumptions. First, we assume coherent and efficient preparation of amplitude-encoded probability distributions, which implicitly requires either quantum-accessible generative models or structured distributions amenable to efficient loading [6,13]. Second, we assume the availability of reversible threshold-marking oracles that identify tail events

without prohibitive overhead. Third, the asymptotic advantage presumes that circuit depth and coherence times scale favorably with the desired precision, allowing the $O(1/\varepsilon)$ query complexity to dominate constant factors.

In addition, discretization plays a critical role: the grid resolution must be sufficiently fine so that discretization error does not mask the gains from improved probability estimation. These assumptions are standard in quantum risk analysis but are essential for translating asymptotic improvements into practical gains.

C. Asymptotic Behavior vs. Simulator Artifacts

While the asymptotic scaling advantages of IQAE and QSP/QSVT are well established theoretically [4,5,7], several effects observed in our results are attributable to simulator-specific or finite-sample artifacts rather than fundamental limitations. These include localized non-monotonicities in IQAE-based CVaR at very small tail levels, which arise from ratio amplification of estimation error, finite grid resolution, and conservative default IQAE stopping rules. Similarly, small deviations at extreme confidence levels in QSP/QSVT results reflect polynomial approximation error near discontinuities and finite sampling noise.

Such effects are expected to diminish with improved parameter tuning, finer discretization, and increased oracle budgets, and should not be interpreted as violations of the underlying asymptotic guarantees.

D. Future Directions: Customized IQAE Schedules

In this work, all IQAE experiments employed the default k-schedule provided by the implementation, which prioritizes robustness and simplicity. A promising direction for future work is to design *customized k-schedules* tailored to tail-risk estimation. Adaptive or problem-aware schedules could reduce variance in small-α regimes, mitigate ratio-instability in CVaR and EVaR, and improve practical convergence without increasing asymptotic cost.

Additionally, exploring hybrid strategies may further enhance stability and efficiency. These directions are particularly relevant for near-term quantum devices, where circuit depth, coherence, and measurement cost remain tightly constrained.

References

[1] Artzner, P., Delbaen, F., Eber, J.-M., & Heath, D. (2001). Coherent Measures of Risk. *Mathematical Finance*, 9(3), 203–228. https://doi.org/10.1111/1467-9965.00068

[2] Bahadur, R. R. (1966). A Note on Quantiles in Large Samples. *The Annals of Mathematical Statistics*, 37(3), 577–580. https://doi.org/10.1214/aoms/1177699450

[3] Metropolis, N., & Ulam, S. (1949). The Monte Carlo Method. *Journal of the American Statistical Association*, 44(247), 335–341. https://doi.org/10.1080/01621459.1949.10483310

[4] Brassard, G., Høyer, P., Mosca, M., & Tapp, A. (2000). Quantum Amplitude Amplification and Estimation. *arXiv preprint* arXiv:quant-ph/0005055. https://arxiv.org/abs/quant-ph/0005055

[5] Grinko, D., Gacon, J., Zoufal, C., & Woerner, S. (2021). Iterative quantum amplitude estimation. *npj Quantum Information*, 7, 52. https://doi.org/10.1038/s41534-021-00379-1

[6] Woerner, S., & Egger, D. J. (2019). Quantum risk analysis. *npj Quantum Information*, 5, 15. https://doi.org/10.1038/s41534-019-0130-6

[7] Montanaro, A. (2015). Quantum speedup of Monte Carlo methods. *Proceedings of the Royal Society A*, 471(2181), 20150301. https://doi.org/10.1098/rspa.2015.0301

[8] Perl, Y., Itai, A., & Avni, H. (1978). Interpolation search—a log log N search. *Communications of the ACM*, 21(7), 550–553. https://doi.org/10.1145/359545.359557

[9] National Institute of Standards and Technology (NIST). Cumulative Distribution Function of the Standard Normal Distribution. *NIST/SEMATECH e-Handbook of Statistical Methods*. https://www.itl.nist.gov/div898/handbook/eda/section3/eda3671.htm

[10] Kao, LJ., Lee, CF. & Lee, HH. (2025). Estimated Sharpe ratio of asset returns with fat tails: theory and empirical evidence. *Rev Quant Finan Acc*. https://doi.org/10.1007/s11156-025-01474-6

[11] Bignozzi, V., Tsanakas, A., & Wüthrich, M. (2024). A credibility framework for extreme Value-at-Risk. *Decisions in Economics and Finance*. https://doi.org/10.1007/s10203-024-00425-6

[12] Dutta, K., & Babbel, D. (2012). On measuring skewness and kurtosis in short-term financial returns using the Pearson Type IV distribution. *Journal of Financial Economic Policy*. https://ideas.repec.org/a/eee/finana/v22y2012icp10-17.html

[13] Laudagé, C., & Turkalj, I. (2022). Quantum Risk Analysis: Beyond (Conditional) Value-at-Risk. https://arxiv.org/pdf/2211.04456

[14] Stamatopoulos, N., Clader, B. D., Woerner, S., & Zeng, W. J. (2024). Quantum Risk Analysis of Financial Derivatives. https://arxiv.org/pdf/2404.10088